UNIVERSITYOF BIRMINGHAM

University of Birmingham
Research at Birmingham

Interactions between aftertreatment systems architecture and combustion of oxygenated fuels for improved low temperature catalysts activity

Fayad, Mohammed; Fernandez-Rodriguez, David; Herreros, Jose; Lapuerta, M; Tsolakis, Athanasios

Link to publication on Research at Birmingham portal

Interactions Between Aftertreatment Systems Architecture and Combustion of Oxygenated Fuels for Improved Low Temperature Catalysts Activity

M.A. Fayad[a,b], D. Fernández-Rodríguez[c], J.M. Herreros[a], M. Lapuerta[c], and A. Tsolakis[a*]

[a] School of Engineering, Mechanical Engineering Department, University of Birmingham, Edgbaston, Birmingham B15 2TT, UK

[b] Energy and Renewable Energies Technology Center, University of Technology, Baghdad, Iraq

[c] University of Castilla-La Mancha, Escuela Técnica Superior de Ingenieros Industriales, Edificio Politécnico. Avda. Camilo José Cela s/n, 13071 Ciudad Real, Spain

* Corresponding author. tel.: +44 (0) 121 414 4170; a.tsolakis@bham.ac.uk

Abstract

Diesel engine vehicles, despite their good fuel economy and reduced CO_2, are receiving significant attention and negative publicity in recent years due to their difficulties in achieving the emissions regulations. This has widely been linked to undesirable environmental impact and health effects.

The lower exhaust gas temperatures associated with modern and more efficient hybrid powertrain and diesel engines makes current technology catalytic aftertreatment systems less efficient under range of vehicle operating conditions. This study, demonstrates how changes in the commonly used aftertreatment system architecture and changes in fuel composition in this case through the addition of oxygenated fuels (i.e. butanol) in diesel fuel can provide meaningful low temperature catalyst activity improvements.

The catalyst oxidation kinetics of CO and HC species were improved (reduced the light-off temperature by around 20 ℃) when a diesel particulate filter (DPF) was placed upstream of the DOC, while the combination of DPF and combustion of oxygenated fuel in diesel led to up to 80 ℃ improvement in catalyst activity. The prevention of soot reaching the DOC active sites increases the rate of reactions and the species accessibility to the active sites of the catalyst, and thereby the oxidation of emissions (CO, HC, and NO) can occur at lower catalyst temperatures. The combustion of diesel-butanol blend further improved the DOC low temperature activity. The major contributors to the improved catalyst light-off, are the reduced level of soot and hydrocarbon emissions as well as the higher reactivity of the hydrocarbons species emitted under butanol blend combustion.

Keywords: butanol, aftrertreatment synergies, aftertreatment architecture, catalyst activity, diesel oxidation catalyst, diesel particulate filter, particulate matter, pollutant emissions.

Graphical Abstract (G.A):
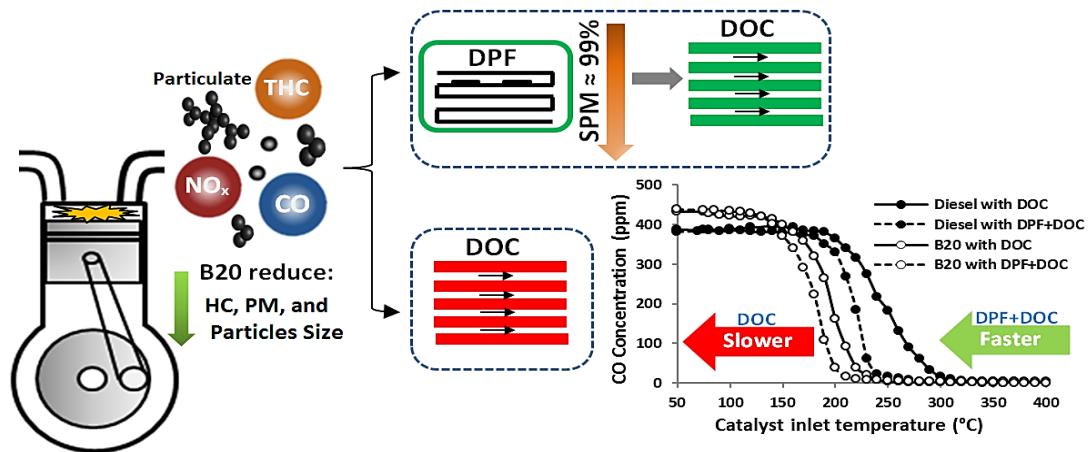
1. Introduction

Modern diesel engine vehicles provide lower fuel consumption, reduced gaseous emissions, and good driving performance. However, nitrogen oxides (NO_x) and particulate matter (PM) emissions emitted form diesel vehicles have been recognized as a major concern for public health and contribute to respiratory cardiovascular diseases [1, 2]. The marginal improvements on pollutant emissions from the combustion of fossil fuels when the engine mapping and/or the engine design is modified has led to the extensive research on aftertreatment systems and alternative transportation fuels as ways of meeting the stringent passenger vehicle tailpipe emission regulations [3].

Bioalcohol fuels can improve engine emissions when used in fuel blends with petroleum diesel fuels [3]. The hydroxyl group of the alcohol molecules reduces unburnt total hydrocarbons (THC) and carbon monoxide (CO) as well as soot formation and, in consequence, particulate emissions [4, 5]. Alcohol fuels tend to reduce NOx emissions due to their high heat of vaporisation and their water content [4, 5], while their low cetane number could increase NOx emissions [4]. Therefore, the overall effect will depend on engine technology and engine operation condition. The reported drawbacks with the ethanol-diesel blends such as poor solubility with diesel [6], lower viscosity [7] and lower lubricity [8, 9] can be partially resolved with the use of butanol-diesel blends [9]. Longer chain alcohols provide more stable fuel blends at low temperature due to their higher solubility in diesel fuels. Furthermore, butanol has higher heating value, higher cetane number [10] and it is less volatile [11], less hydrophilic and also less polar than other lighter alcohols. However, more studies are needed to assess its energy intesity and green gas house emissions in life cycle analysis, its availablity to replace a realistic share of diesel fuel in the current market and the enhaced biological activity of its exhaust gas as reported in [12].

Aftertreatment systems can include sophisticated technologies such as a diesel oxidation catalyst (DOC) and diesel particulate filter (DPF) [13] or hybrid technologies such as DOC and NOx control catalysts coated on the DPF [14]. DOCs with high cell density (large surface area) and enough

loading of catalytic materials such as platinum and/or palladium are able to almost eliminate CO and THC under certain conditions (i.e. [15, 16]). DPF is an effective PM trapping and reduction aftertreatment system [17, 18]. The introduction of a DOC upstream of the DPF in combination with post-injection can aid DPF active regeneration by increasing exhaust gas temperature with the combustion of post-injected fuel [19] as well as passive regeneration at lower temperature due to the increased NO_2 concentration in the exhaust gas [20, 21].

The DOC efficiency in oxidizing CO, THC and NO depends on the residence time of the exhaust gas in the catalyst, the temperature and the level and nature of the exhaust species and inhibitions/synergies between the different species contained in the exhaust gas [22]. Higher space velocity of the exhaust gas, limits the capacity of the gaseous emissions in reaching and interacting with the coated walls of the DOC [23, 24]. Post-injection in combination with the DOC is used to increase the exhaust gas temperature in order to aid the DPF regeneration (i.e. active regeneration) [25]. Post injection (timing and quantity) impacts engine output emissions [26-29], sharply increasing CO and THC emissions as the late injected fuel is not burnt in the combustion chamber [28], and thus influencing the aftertreatment performance [17]. Overall THC and CO conversion efficiencies with late post injections are lower than that without post injection due to the increased engine-out CO emissions, which inhibits the THC oxidation inside the DOC as well as the generation of long-chain THC species from post injection with limited diffusivity to reach the DOC active sites to be oxidised [16]. Cleaner fuels can enhance the catalyst activity at lower temperatures because they produce lower emissions concentration during combustion (THC, CO and PM) and reduce the competition of species for catalyst active sites [25, 30].

Studies at system level, taking into consideration the combination of fuel properties fuel post-injection strategies, exhaust gas characteristic (i.e. space velocity, emissions concentration, temperature) and aftertreatment systems re-architecture can contribute in fulfilling the forthcoming stringent emission regulations. In this work the light-off activity of a DOC catalyst was studied by manipulating a modern diesel engine exhaust gas composition through the combustion of butanol blending with diesel, fuel post injection strategies, changes in the Gas Hourly Space Velocity (GHSV) and the placement of a DPF upstream the DOC to filter and prevent high molecular weight species such as soot and heavy HC reaching the DOC. The combination of cleaner combustion fuel (i.e. butanol blend) and unconventional aftertreatment architecture (DPF upstream of a DOC) makes more apparent the impact of these carbon species on DOC activity for the case of diesel fuel combustion without upstream DPF.

2. Experimental apparatus, materials and test matrix

2.1 Experimental setup

A single cylinder diesel engine (Table 1) equipped with a high-pressure common-rail fuel injection system that allows the control of pilot injection, main injection, and post-injection (i.e. pressure, injection rate and fuel quantity) has been used in this study. A simplified schematic layout of the experimental set-up is detailed in Figure 1. The engine exhaust is linked to a bespoke catalyst test rig that allows catalyst activity and characterisation studies. The mini reactor was positioned inside a furnace and a sample of the engine exhaust gas was directed to the reactor. The facility allows parameters such as temperature, pressure and space velocity to be selected according to the study requirements. The combined arrangement of DPF and DOC aftertreatment systems is also shown (see Figure 1).

An electric dynamometer with motor and a load cell was used to control the engine load. A digital shaft encoder (producing 360 pulses per revolution) was used to measure the crankshaft position and the pressure transducer mounted at the cylinder head and connected via an AVL FlexiFEM 2P2 charge amplifier was used to measure in-cylinder pressure. To monitor intake air flow rate, pressure, and temperature (oil, air, inlet manifold and exhaust), standard engine test rig instrumentation was used. A bespoke LabVIEW based code was used to perform data acquisition and combustion analysis. Furthermore, the other engine operating parameters, including fuel injection strategy (i.e. post injection timing, main/post injection ratio, and injection pressure) were controlled by using an in-house developed LabVIEW programme. Injection settings are listed in Table 1. Injection duration has been adjusted for each fuel to reach the desired engine operation condition defined by engine speed and indicated mean effective pressure. K-type thermocouples and a TC-08 Thermocouple Data Logger (Pico Technology) were used to measure the engine exhaust temperature [31]. During this work, the engine was running with post-injection and the engine speed was controlled at 1800 rpm for all tests with an engine load of 3 bar indicated mean effective pressure (IMEP). This condition is within a frequent engine speed-load window in vehicle driving cycles as well as it provides representative and stable engine output gaseous emissions and exhaust temperature. The oxidation catalyst was subjected to two exhaust gas space velocity (ratio between volumetric gas flow rate and reference volume of the aftertreatment component [32]) of 25,000 h^{-1} and 50,000 h^{-1} and to a heating temperature ramp of around 2 °C/min during every test.

The conversion efficiency was calculated according to the continuously recorded of exhaust gas concentration at the catalyst. Experimental uncertainty has been calculated and error bars have been added to all the figures. In order to remove any remaining fuel from the previous experiment, the fuel tank and fuel lines were cleaned and the engine was running for 30 minutes with the same fuel.
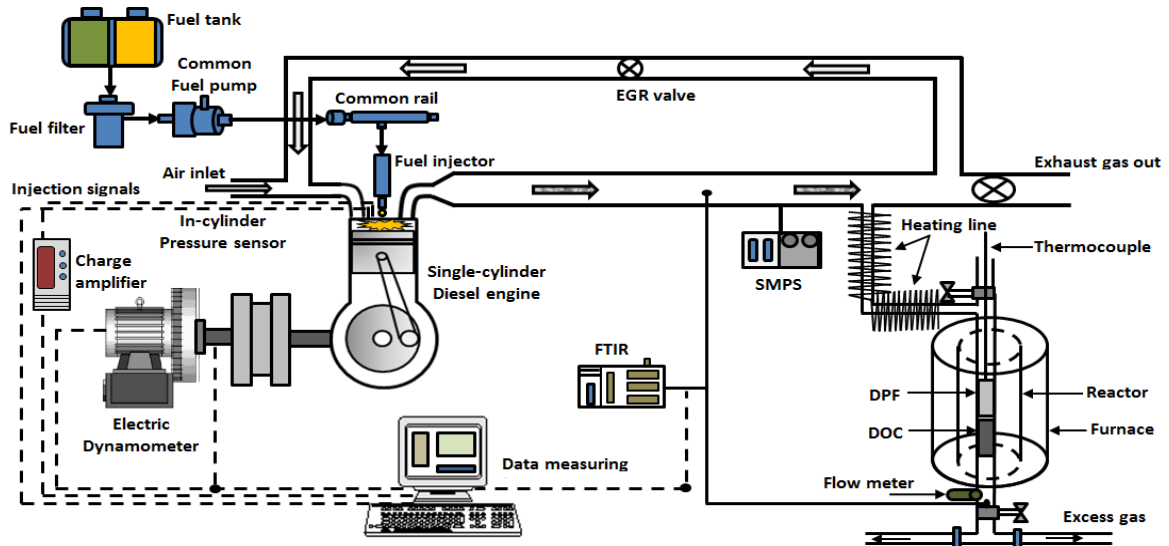
Figure 1: Schematic diagram of experimental test and sampling point.

Table 1. Research engine specifications.

Engine parameters	Specifications
Engine type	Diesel 1- cylinder
Stroke type	Four-Stroke
Number of cylinders	1
Cylinder bore x stroke (mm)	84 x 90
Connecting rod length (mm)	160
Compression ratio	16.1
Displacement (cm^3)	499
Injection system	Common rail
Fuel pressure range (bar)	500-1500
Pre, main and post injection timing	15, 3 and -60 deg bTDC
Number of injections	3 injection events

2.2 Emissions instruments and catalyst

A MultiGas 2030 FTIR (Fourier transform infrared) spectrometry technique was used to measure exhaust emissions including: nitrogen oxides (NO and NO_2), nitrous oxide (N_2O), water (H_2O), formaldehyde (CH_2O), carbon dioxide (CO_2), carbon monoxide (CO) and individual light hydrocarbons species including methane (CH_4), ethane (C_2H_6), propane (C_3H_8), ethylene (C_2H_4), propylene (C_3H_6) and acetylene (C_2H_2). The SMPS (scanning mobility particle sizer, model TSI/3080) composed by electrostatic classifier, a 3081 DMA (Differential mobility analyser), and a 3775 CPC (Condensation particle counter) was used to study the particle size distribution (PSD) in the exhaust gas. The sheath flow rate and aerosol flow rate were set at 6.00 L/min and 0.60 L/min respectively to provide a PSD range between 10.4 nm and 378.6 nm. A small portion of the exhaust gas was sampled and diluted with air and the dilution ratio was set at 1:100 at constant air dilution temperature (150 ℃). The SMPS was

connected downstream of the dilution system to extract a diluted sample for the particle size measurement.

The engine exhaust gas composition was measured at regular intervals during the tests. The outlet exhaust gas composition of DOC was continuously recorded throughout the experiment, while the temperature at the DOC inlet was varied from 50 °C to 400 °C. The engine tests were carried out to explore how the hydrocarbons produced from the post-injection working with two different fuels influence the DOC performance. The catalysts were placed inside a mini-reactor (DPF + DOC) and they were fed with actual exhaust gas produced by the engine. The DOC was loaded with platinum-palladium (weight ratio 1:1). It is composed of an alumina and zeolite washcoat and coated on a cordierite honeycomb monolith (25.4 mm x 91.4 mm) and 4.3 mil wall thickness, with dimensions of 0.258 cells per m^2. The diameter and length of DPF are 24.2 mm and 75.2 mm respectively with a channel density of 289 cpsi.

2.3 Fuels and blends

The fuel specifications and properties are listed in Table 2. The diesel fuel was supplied by Shell Global Solutions UK and the butanol (used in blending) was from Fisher Scientific Company. Particularly, the diesel fuel used as reference was selected without any biodiesel (no oxygen content) in its composition. The butanol fuel has high purity of 99%. The fuel blend (diesel-butanol) was composed of 80% diesel and 20% butanol (%vol.)

Table 2. Specification of tested fuels [25, 33].

Properties	Method	Diesel	Butanol	B20
Derived cetane number	ASTM D7668-14	50.2	17	41.98
Latent heat of vaporization (kJ/kg)		243	585	-
Bulk modulus (MPa)		1410	1500	-
Density at 15 °C (kg/m^3)	EN 12185	840.4	809.5	833.2
Upper heating value (MJ/kg)		45.76	36.11	43.5
Lower heating value (MJ/kg)		43.11	33.12	40.91
Water content by coulometric KF (mg/kg)	EN 12937	40	170	389.4
Kinematic viscosity at 40 °C (cSt)	EN ISO 3104	2.564	2.23	2.27
Lubricity at 60 °C (μm)	EN ISO 12156	424	571.15	444.5
Fatty acid methyl ester % (v/v)	NF EN 14078-A	<0.05		
Cold filter plugging point (CFPP)	ASTM D-6371	-18	<-51	-18
C (wt %)		86.44	64.78	81.56
H (wt %)		13.56	13.63	13.35
O (wt %)		0	21.59	4.318

3. Results and discussions

3.1 Influence of fuel on PM and gaseous emissions

In this section, the effect of butanol blend fuelling on engine particulate matter and gaseous emissions was analysed under post fuel injection strategy.

Particle size distribution (PSD): Figure 2 shows particle number concentrations and particle size distributions for Diesel and B20 measured from the engine exhaust. Lower particle number concentrations were observed when B20 was used, as well as a lower mean particle diameter. The average particle diameters were 79.71 nm for diesel and 74.81 nm for B20. The main reason for the reduction in the particle number is the oxygen content in the butanol molecule, which promotes soot oxidation from the internal bond-oxygen, leading to the elimination of most of the soot primary particles previously formed, and to the reduced size of the remaining particles [34, 35]. In addition, the reduction in the particle concentration contributes to reduce the probability of collisions between particles, thus further producing smaller agglomerates compared to the diesel fuel, in agreement with previous studies with alcohol blends [30, 36].
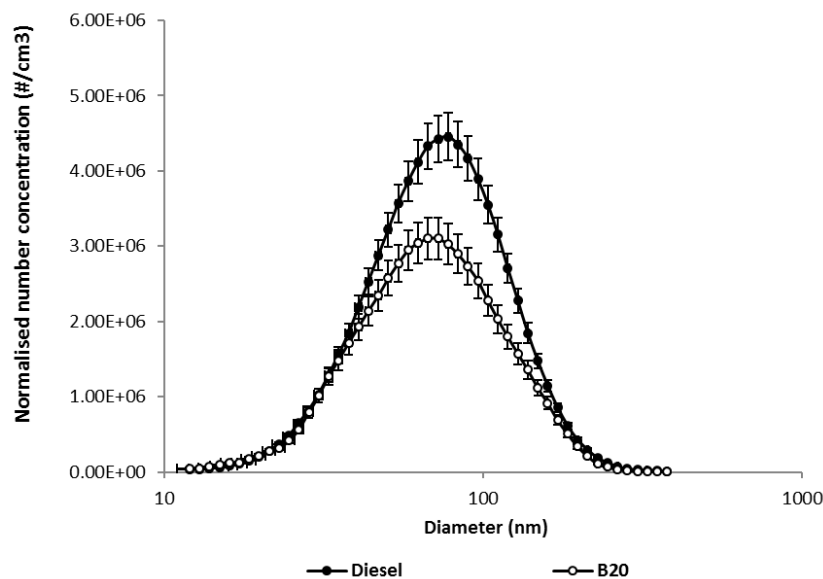

Figure 2. Effect of fuel on particle size distribution.

Engine output gaseous emissions: The effect of fuel properties on gaseous emissions for diesel and butanol blend are shown in Table 3. NO_X emissions remain constant independently of the fuel used. It is thought that the potential increase of NO_X due to the lower cetane number and presence of the internal oxygen in the butanol molecule is compensated by a reduction in local temperature because of butanol's higher enthalpy of vaporization. However, a slight increase in the NO_2 emissions from the combustion of B20 was observed [37] as compared to the diesel fuel combustion, effect that has been also described by Chen et al. [38] and Fayad et al. [35]. CO emissions increase slightly and THC emissions decrease when B20 is used instead of diesel fuel. The presence of butanol in the blend has a twofold effect: on

7

the one side, internal oxygen enhances combustion efficiency and, as a consequence THC emissions decrease with respect to diesel fuel combustion. However, these THC emissions could not be completely oxidised to CO_2, leading to partially oxidised CO, because of the higher vaporization enthalpy of the alcohol. For a more comprehensive analysis of the THC, some relevant light saturated hydrocarbons (methane and ethane) and unsaturated hydrocarbons (ethylene, propylene, acetylene) species have been analysed independently, while the rest of species have been grouped as heavy hydrocarbons (HHCs). Table 4 shows that HHCs, which represent around 65% of THCs for both fuels, have the same tendency as THC. However, a higher level of light HCs species (saturated and unsaturated) can be observed from the combustion of the butanol blend (B20) compared to diesel fuel, which could influence the DOC light-off [38]. This is likely to be a result of the butanol's thermal decomposition to light HC species and CO while in case of diesel fuel combustion it produces heavier HC components.

Table 3. Engine output emissions at 1800 rpm and 3 bar IMEP.

Engine output concentration (ppm)	Diesel	B20
Nitric oxide (NO)	164	160
Nitric dioxide (NO_2)	44	51
Nitrogen oxides NO_X	208	211
Carbone monoxide (CO)	391	475
Total hydrocarbons (THCs)	1129	890
Heavy hydrocarbons (HHCs)	758	571
Methane (CH_4)	6	8
Ethane (C_2H_6)	5	6
Acetylene (C_2H_2)	4	5
Ethylene (C_2H_4)	22	27
Propylene (C_3H_6)	8	9
Formaldehyde (HCHO)	24	26

3.2 Effect of fuel combustion and DPF incorporation on the DOC light-off

In this section the effect of B20 and diesel fuel combustion on the DOC light-off performance has been analysed with and without a DPF. The incorporation of a DPF upstream of the DOC implies removing large part of the soot and heavy hydrocarbons from the exhaust before they reach the oxidation catalyst. As previously reported, the DPF can trap more than 99% of solid PM (SPM) by mass and number from a diesel engine exhaust derived from diesel and oxygenated fuel combustion [15]. The prevention of soot and of HHCs reaching the DOC could improve transport limitations of the reactants to the active sites and will allow a better adsorption of gaseous emissions into the active sites of the DOC. Furthermore, these tests add further understanding to identify and evaluate the

different factors which contributed to the improved catalyst oxidation activity previously reported with B20 engine fuelling with respect to diesel fuel combustion.

DOC ability to oxidise CO and THCs: Figures 3 and 4 show that the DOC is more efficient in oxidising CO and THC, respectively when the DPF is introduced upstream of the DOC for both studied fuels. Particularly, the placement of the DPF upstream of the DOC and the use of B20 improved the CO catalyst light-off by up to around 70 °C (temperatures are considered when catalyst reach 50% conversion efficiency) as well as increase the CO and THC oxidation rate with increasing temperature when compared to diesel fuel combustion. It can be noticed that the oxidation of the THC was not complete over the DOC and their oxidation started at higher temperature than that of CO, especially for the combustion of diesel fuel without the use of the upstream DPF. This is probably due to incomplete conversion for some of HC species, which are difficult to oxidise over the catalyst. Potential condensation of heavy hydrocarbons enhanced through the presence of zeolite within the catalyst's washcoat enable to trap medium-heavy hydrocarbons at low temperature, being released at higher temperature [16, 29] and as discussed later.

Therefore, the DOC's light-off temperature is highly dependent on the exhaust gas composition, as the cleaner combustion of B20 and the filtering of the exhaust gas with the DPF shifted CO and THC light-off towards lower temperatures and steeper conversion efficiency. The results shown in Figures 3 and 4 enable to differentiate the effects of active sites availability (e.g. different particle and THC concentration levels upstream of the DOC) with respect to the effect of the different diffusivity and reactivity between the combustion products. It is obtained that the negative effect of particle and heavy hydrocarbons blocking the active sites influence the catalyst activity for both fuels, but being more influential for diesel exhaust with respect to B20. From the comparison between the DOC catalytic activity with the DPF for both fuels, the following factors contribute to the improved catalyst light-off and steeper conversion efficiency with increasing catalyst temperature with B20: (i) the higher reactivity and diffusivity of butanol and its combustion products [9, 25], (ii) the lower THC concentration upstream of the catalyst and (iii) the higher NO_2 concentration in the exhaust gas [9, 35]. Factors i and ii enhance the active site availability and reduce the competition for active sites [24, 28], whereas factor iii increases the oxidation potentially.
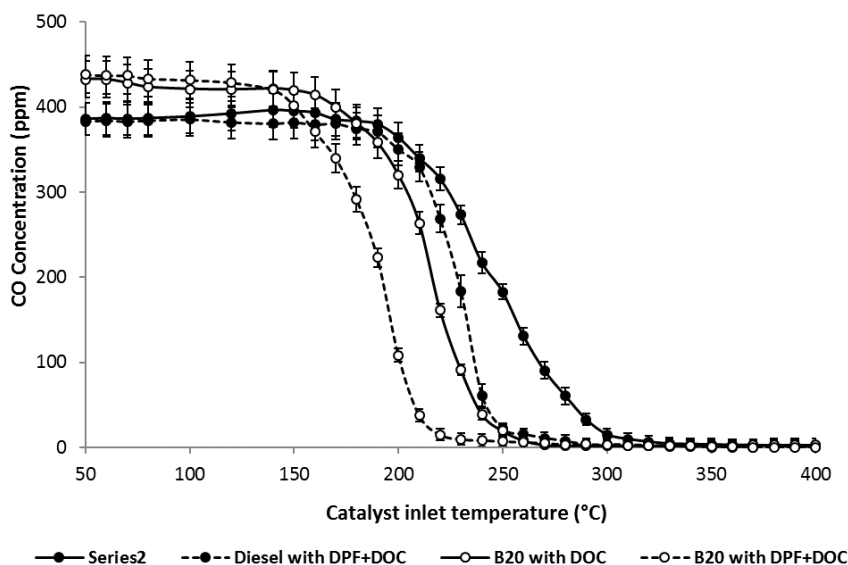
Figure 3. CO oxidation light-off temperature in the DOC (with and without DPF) for diesel and B20 fuels.
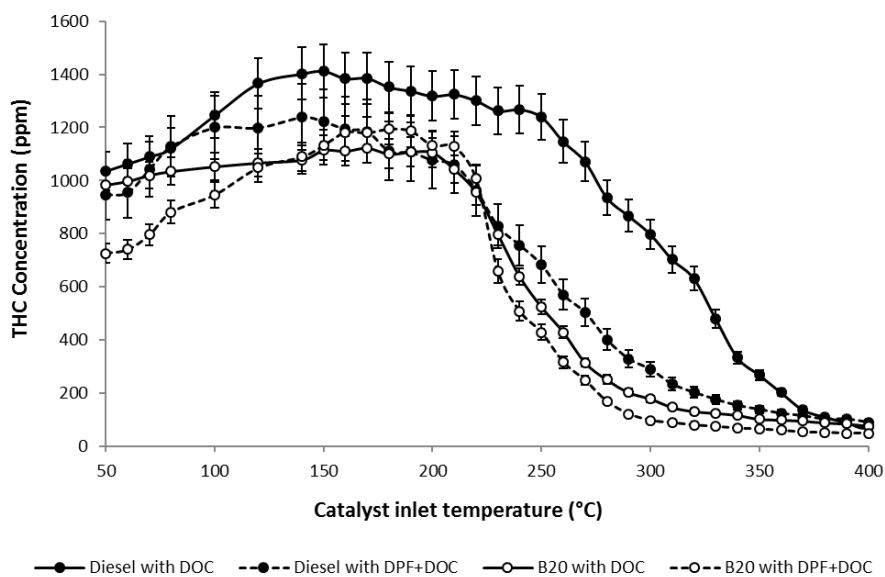

Figure 4. THC oxidation (light-off) temperature in the DOC (with and without DPF) for diesel and B20 fuels.

DOC ability to reduce the individual HCs species: The conversion of the individual HC species in the DOC from the combustion of diesel and B20 are presented in Figure 5. The incorporation of the DPF upstream the DOC, also reduces the light-off temperature for the individual HC species (Figure 5, b-g). The individual hydrocarbon species light-off from the combustion of B20 started earlier than those obtained for diesel fuel. The oxidation process of the individual HC species in the DOC started with acetylene, followed by propylene and then the rest of HC species (Figure 5, b-g). In the studied temperature range methane was not oxidised or affected by the differences in the exhaust gas

10

composition, proving that higher exhaust gas temperature would be required (Figure 5-a). Furthermore, the presence of some long chain hydrocarbons classified as "HHC" contribute to the incomplete conversion of THC, resulting from their reduced diffusivity to reach the catalyst active sites [29]. This sequence in hydrocarbon oxidation, with short chain saturated hydrocarbons being the most difficult to oxidise, agrees with the results reported by Diel et al. [39] and Herreros et al. [16]. From the results, it can be concluded that the same factors and contributions to the case of CO and THC emissions also apply to the oxidation of the individual hydrocarbon species [39].
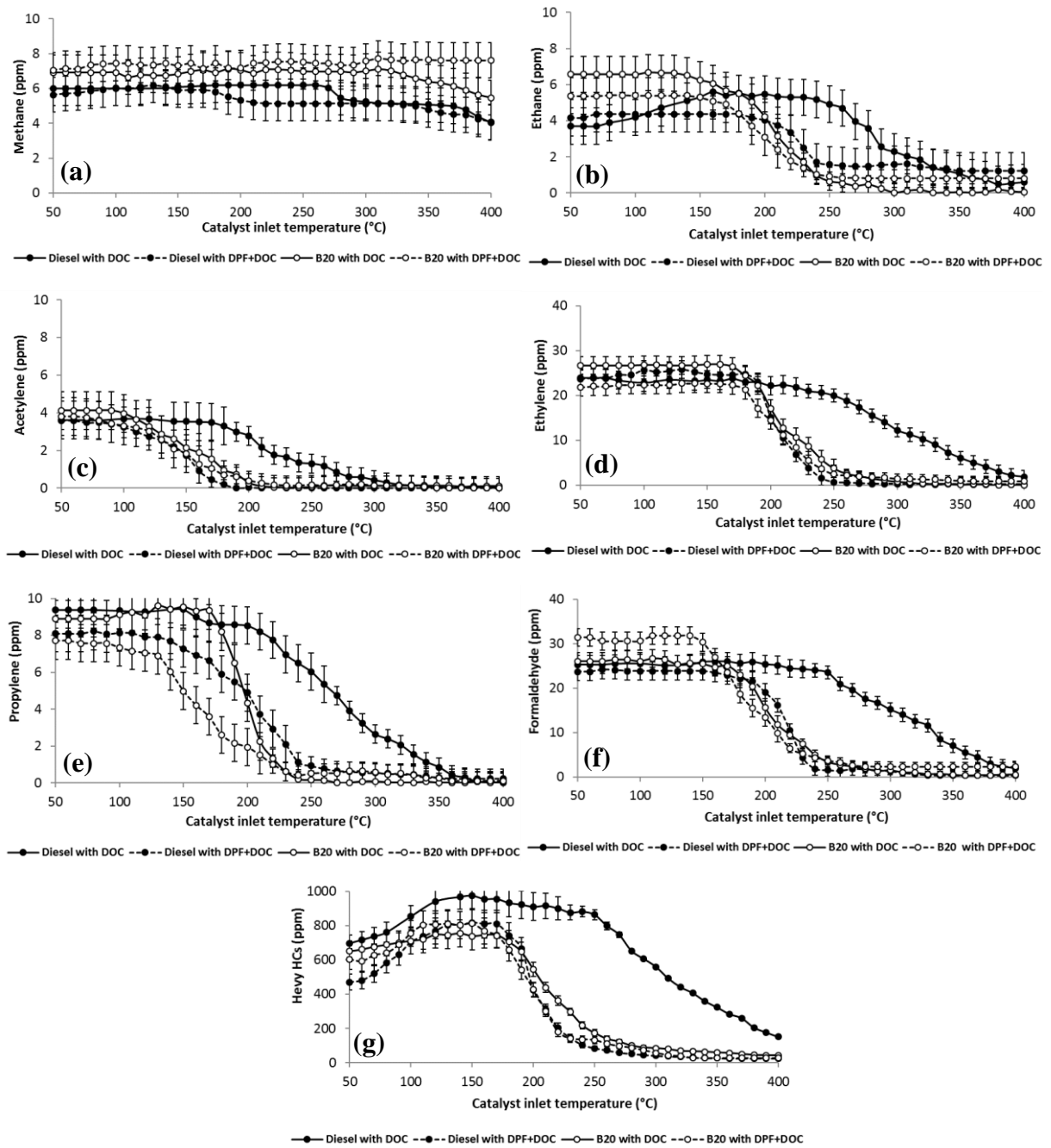

Figure 5. Hydrocarbon species light-off temperature in the DOC (with and without DPF) for diesel and B20 fuels (a) methane, (b) ethane, (c) acetylene, (d) ethylene, (e) propylene, (f) formaldehyde, (g) HHCs.

DOC ability to oxidise NO/NO$_2$: NO$_2$ concentration in the untreated exhaust is dependent on the fuel used and engine operation (i.e. load, air/fuel ratio and fuel injection strategies). A higher ratio of NO$_2$/NO upstream of the DOC can be observed from the combustion of B20 (Table 3), trend also reported in [16]. Pioneering work by Murakami et at. [40, 41]investigated several additives, including CH$_3$OH, H$_2$, H$_2$O$_2$, CH$_2$O, CH$_4$, and they found that the degree of NO to NO$_2$ conversion was dependant on the production rate of peroxyl (HO$_2$) radicals during the combustion process of the additives. Hjuler et al. [42] using a laboratory scale reactor, proved that at a specific temperature window a simultaneous oxidation of the organic compounds and NO to NO$_2$ occurs, results already observed in catalytic processes in vehicles [43, 44]. The oxygenated organic compounds such as methanol, methylamine, acetaldehyde, acetone and ethane were found to affect the rate of NO to NO$_2$ conversion but also the width of the temperature window for oxidation. They reported that the efficiency of a given compound in oxidizing NO could be attributed to its oxidation mechanism as it depends on the production of peroxyl radicals, HO$_2$. Parameters such as the ratio of organic compounds to NO, reaction temperate, reaction time, and presence of water were all found to influence the NO to NO$_2$ oxidation [42]. For example, methanol/NO ratio of around 1 provided high NO to NO$_2$ promotion efficiencies i.e. (80% to 90%), while at lower molar ratios the conversion was reduced.

A CFD investigation by Zhang et al. [45] and Lilik et al. [46] confirmed that combustion temperature changes alone are not sufficient to explain the increase in NO$_2$ with increasing H$_2$. Their CFD results are also consistent with the hypothesis that in-cylinder HO$_2$ enhances the conversion of NO to NO$_2$ in the diesel engine exhaust. This trend that was seen here with the introduction of butanol in diesel combustion, where the OH in the oxygenated fuels can increase the OH$_2$ radicals in the combustion process and thus promote the formation of NO$_2$.

The DOC catalyst is usually designed to promote the NO to NO$_2$ conversion [47-49] in order to enhance the low temperature passive soot oxidation. However, this reaction is also influenced by the concentration of CO and the type of THC in the catalyst [16, 29]. The production of NO$_2$ is temperature dependant, with approximately 250 °C being the starting temperature for the DOC under investigation for both fuels. It is thought that at low temperature, the engine out NO$_2$ emissions of approximately 44 and 50 ppm from the diesel and B20 combustion (see Table 4) is preferentially used to oxidize HCs in the DOC. The presence of the DPF upstream of the DOC also enhances the NO$_2$ production in the DOC for diesel fuel. This can be attributed to a) the reduced reaction rates of the NO$_2$ production of carbon-containing species and b) the enhanced catalyst oxidation activity, as evidenced from the earlier CO and HC light-off curves, due to the improved reactant and products transport to and from the active sites, respectively, due to the reduction in carbon species reaching the DOC [49, 50]. The improved CO and THC oxidation with the incorporation of the DPF, does not promote the increase in the NO$_2$ emitted to the atmosphere. The higher CO and THC oxidation when the DPF is introduced, led to higher consumption O$_2$ and NO$_2$. As reported above, work by Hjuler et

al. [42] has shown that reducing the ratio between the NO_2 enhancing additives and the NO emissions can also slow down the NO_2 production. Higher NO_2 concentration was observed downstream of the catalyst from B20 combustion with increasing catalyst temperatures due to a higher oxidation of NO to NO_2, while NO concentration was reduced downstream of the catalyst with respect to the inlet value (Figure 6). In case of using Ag/Al_2O_3 catalyst, a similar effect has been already reported, where the formation of NO_2 is highly promoted under the addition of alcohol fuels [25].
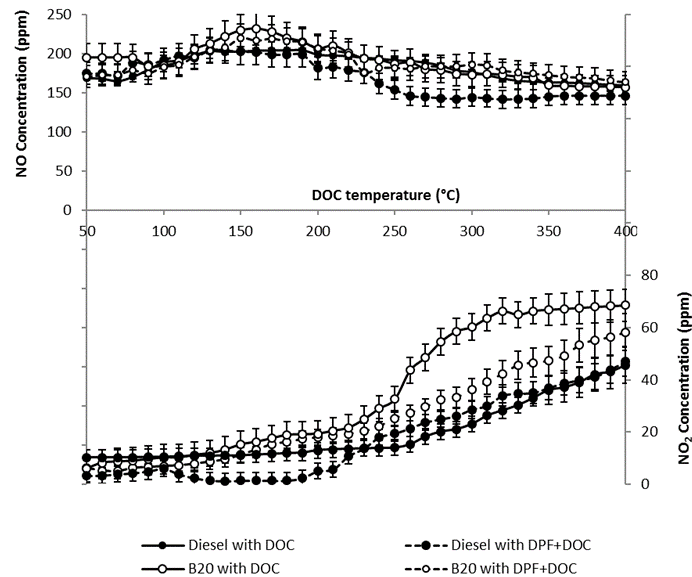

Figure 6. NO to NO_2 oxidation in the DOC (with and without DPF) for diesel and B20 fuels.

3.3 Effect of fuel and flow rate over DOC performance light-off

In this section the effects of B20 and diesel fuel combustion over the DOC light-off performance with an upstream DPF is analysed with different flow rates (i.e. space velocities) (Figure 7). This allows to investigate the effect of the residence time of the exhaust products on their adsorption and oxidation in the DOC active sites at a temperature range from 50 °C to 400 °C.

CO and THC oxidation over DOC at different space velocity (SV): The DOC light-off temperatures for CO and THC oxidation are higher (with a difference of around 30 °C for CO and 40 °C for THC) when the space velocity (SV) was increased from 25,000 h^{-1} (LSV) to 50,000 h^{-1} (HSV) for both fuels. The difference is likely to be a consequence of the shorter time available between the catalyst active sites and exhaust species [21, 24, 49, 50] to diffuse and undergo the oxidation reactions. B20 still maintains an earlier CO and THC light-off with respect to those obtained with diesel fuel combustion. As it was discussed in the previous section, the low THC emissions derived from B20 combustion, as well as the presence of oxygen in the butanol molecule and the higher diffusivity and reactivity of its combustion products favour the accessibility and reaction of CO and THC in the catalyst active sites [51].
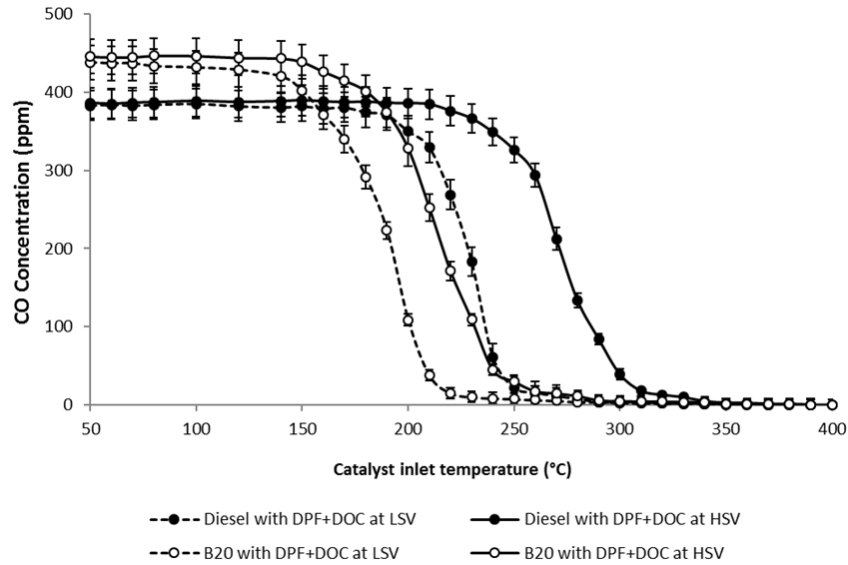
Figure 7. CO oxidation light-off temperature in the DOC at different space velocities for diesel and B20 fuels.
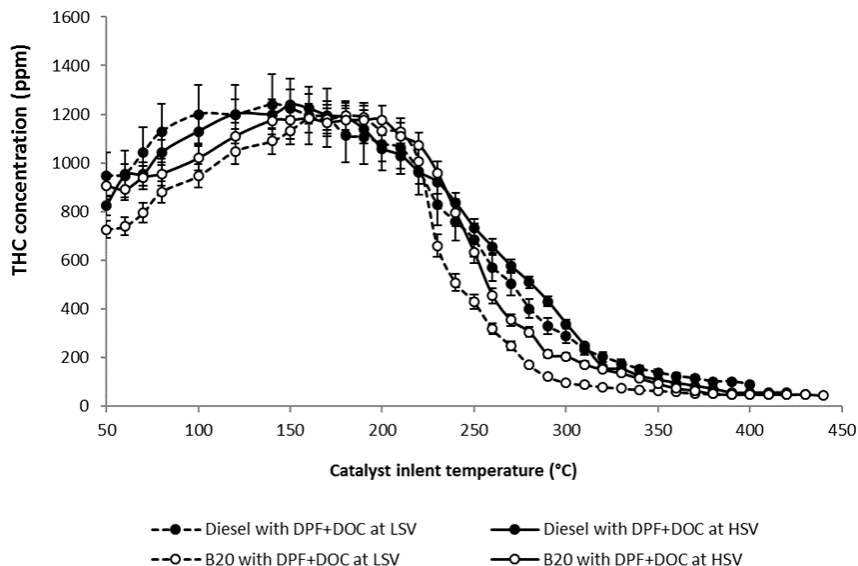

Figure 8. THC oxidation light-off temperature in the DOC at different space velocities for diesel and B20 fuels.

HCs species oxidation over DOC at different SV: The concentration of the individual HC species and HHCs downstream of the DOC at both space velocities is shown in Figure 9. Accordingly to the catalyst light-off temperatures, the oxidation rate of HC species was slower at HSV for both fuels as a result of limited residence time of the exhaust gas within the catalyst. For both SV, the unsaturated HCs are oxidised at lower temperature than saturated ones, a trend that agrees with [52]. Eventually, at both space velocities the DOC oxidised those light HC species except CH_4. At high space velocity, the conversion efficiencies in the case of B20 operation are similar to those obtained with diesel for most of the HC species. Therefore, with the exception of acetylene, it seems that the earlier catalyst

14

light-off for B20 with respect to diesel fuel does not happen at high space velocity, with the exception of acetylene (Figure 9).
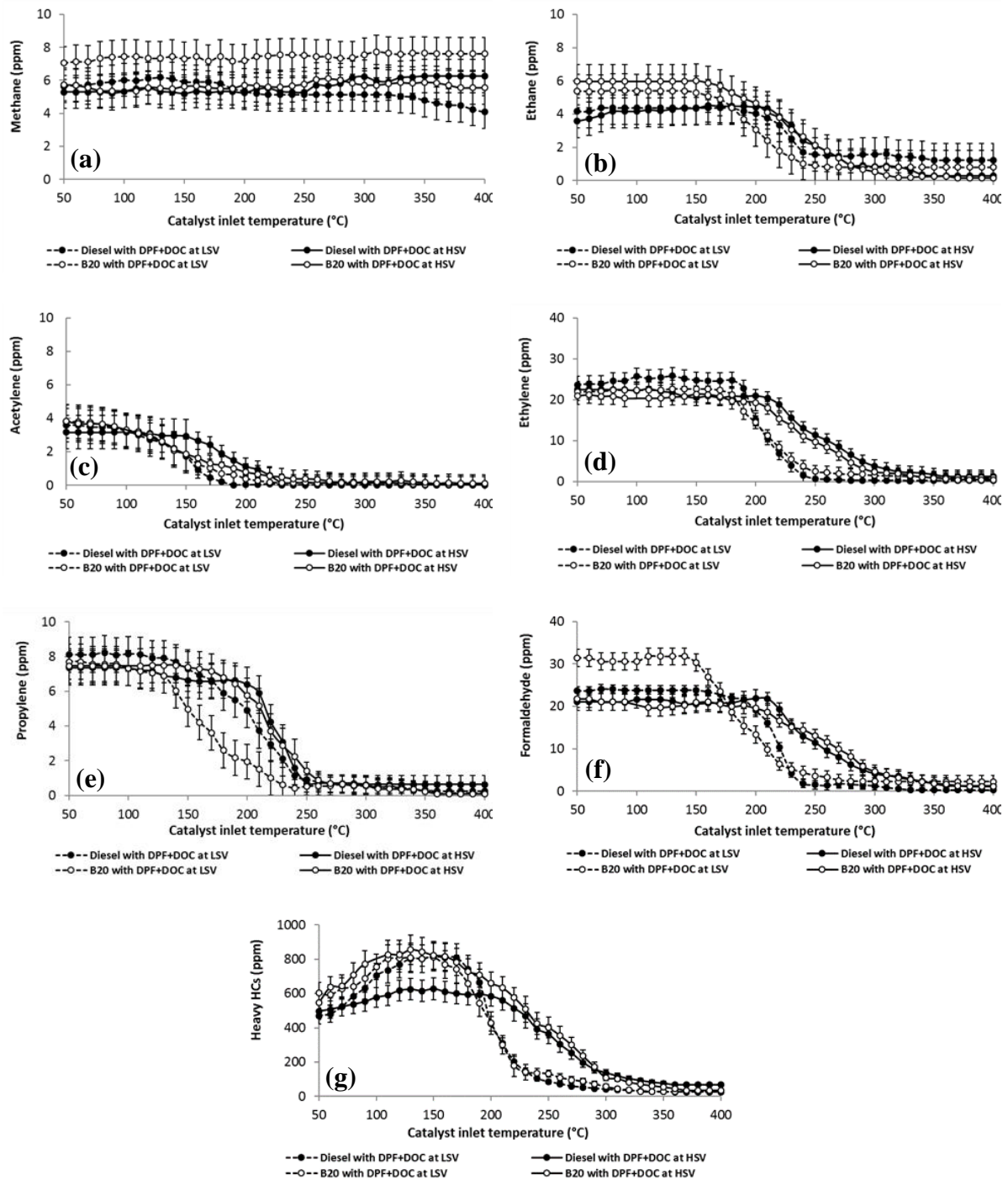

Figure 9. Hydrocarbon species light-off temperature in the DOC at different space velocities for diesel and B20 fuels (a) methane, (b) ethane, (c) acetylene, (d) ethylene, (e) propylene, (f) formaldehyde, (g) HHCs.

NO/NO₂ oxidation over DOC at different SV: For both fuels the NO_2 production was promoted more at low space velocity (Figure 10), which is in accordance with the oxidation of the carbon-containing species. This trend confirms the findings that oxidation of the organic compounds and NO to NO_2 occurs simultaneously [42]. The same authors have also suggested that reduced reaction time (i.e.

15

increased space velocity) also reduces the production of OH_2 radicals and hence NO_2 production. The effect of space velocity is even more pronounced at high temperature when the concentration of NO_2 increases as the formed NO_2 is not consumed in THC oxidation, which reacts preferably with molecular oxygen when the temperature increases [25, 53, 54]. Furthermore, for both SV's the NO to NO_2 oxidation over DOC is slightly higher for B20 than for diesel fuel, due to the higher reactivity and diffusivity of the combustion products of B20 in comparison to diesel fuelling, which enhance the oxidation rate over catalyst [51].
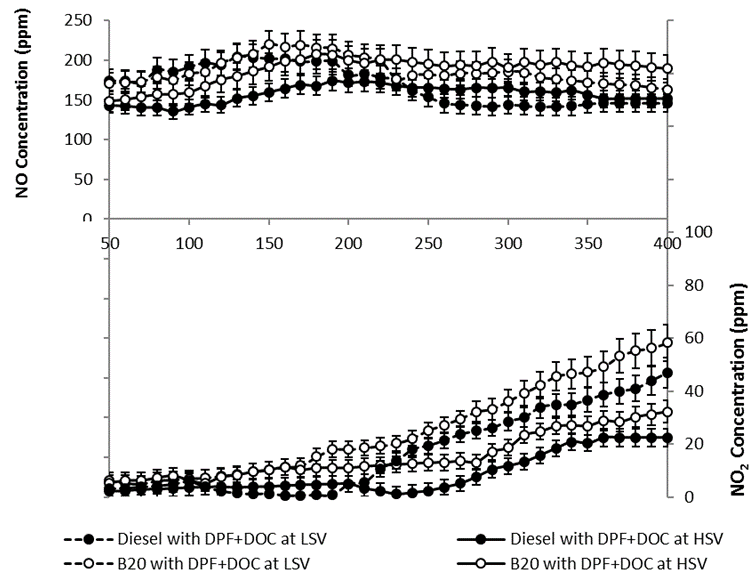

Figure 10. NO/NO_2 oxidation light-off temperature in the DOC at different space velocities for diesel and B20 fuels.

4. Conclusions

Through fuel blending and aftertreatment systems architecture the engine exhaust gas composition can be manipulated in order to improve catalysts activity especially at low temperatures. The absence of solid particles in the exhaust gas and the control of some of the heavy HC species played a key role in improving the oxidation catalyst light-off temperature and enhancing the oxidation rate of CO, THC, and individual HC species at low temperatures by easing accessibility to the active sites of the catalyst (i.e. avoiding masking).

The increased NO_2 during the combustion of oxygenated fuels (i.e. butanol) but also in the DOC indicates that the production of species such as OH_2 radicals can be promoted in diesel engine by the use of some oxygenated fuels additions, work that is in agreement with non-engine studies.

Our finding can be used to guide the design of both more efficient compact aftertreatment systems architecture and cleaner fuels. By identifying the role of the individual species (i.e. reaction promoter, spectators or distractor) during the combustion process and catalytic processes, fuels composition, engine operation and catalyst design and architecture can be optimised. Improved

catalyst activity can also be translated in the design of catalytic technologies with reduced platinum group metals and overall cost or more efficient catalytic systems at urban driving conditions.

5. Acknowledgements

ABBREVIATIONS

B20 = butanol 20 %, and diesel 80 %

CO = carbon monoxide

CO_2 = carbon dioxide

DOC = diesel oxidation catalyst

DPF = diesel particulate filter

GHSV = gas hourly space velocity

HC = hydrocarbons

HHCs = heavy hydrocarbons

HSV = high space velocity

IMEP = indicated mean effective pressure

LSV = low space velocity

NO = nitric oxide

NO_2 = nitrogen dioxide

NO_X = nitrogen oxides

PSD = particulate size distribution

PM = particulate matter

SMPS = scanning mobility particle sizer

SPM = solid particulate matter

THC = total hydrocarbons

6. References

1.   Bouchez, M., Dementhon, J.B., *Strategies for the control of particulate trap regeneration*. 2000, SAE Technical Paper. p. 01-0472, doi:10.4271/2000-01-0472.

2. Gill, S.S., Chatha, G.S., Tsolakis, A., *Analysis of reformed EGR on the performance of a diesel particulate filter.* International Journal of Hydrogen Energy, 2011. **36**(16): p. 10089-10099.

3. Liotta, F.J., Montalvo, D.M. , *The effect of oxygenated fuels on emissions from a modern heavy-duty diesel engine.* SAE Technical Paper, 1993: p. 932734, doi:10.4271/932734.

4. Sukjit, E., Herreros, J.M., Dearn, K.D., Garcia-Contreras, R., Tsolakis, A., *The effect of the addition of individual methyl esters on the combustion and emissions of ethanol and butanol -diesel blends.* Energy, 2012. **42**(1): p. 364-374.

5. López, A.F., Cadrazco, M., Agudelo, A.F., Corredor, L.A., Vélez, J.A., Agudelo, J.R, *Impact of n-butanol and hydrous ethanol fumigation on the performance and pollutant emissions of an automotive diesel engine.* Fuel, 2015. **153**: p. 483-491.

6. Armas, O., García-Contreras, R., Ramos, Á., *Pollutant emissions from New European Driving Cycle with ethanol and butanol diesel blends.* Fuel Processing Technology, 2014. **122**: p. 64-71.

7. Lapuerta, M., Rodríguez-Fernández, J., Fernández-Rodríguez, D., Patiño-Camino, R., *Modeling viscosity of butanol and ethanol blends with diesel and biodiesel fuels.* Fuel 2017. **199**: p. 332-338.

8. Xing-cai, L., Jian-Guang, Y., Wu-Gao, Z., Zhen, H., *Effect of cetane number improver on heat release rate and emissions of high speed diesel engine fueled with ethanol–diesel blend fuel.* Fuel, 2004. **83**(14): p. 2013-2020.

9. Lapuerta, M., García-Contreras, R., Campos-Fernández, J., Dorado, M.P., *Stability, lubricity, viscosity, and cold-flow properties of alcohol-diesel blends.* Energy Fuels, 2010. **24**(8): p. 4497-4502.

10. Lapuerta, M., Hernández, J.J., Fernández-Rodríguez, D., Cova-Bonillo, A., *Autoignition of blends of n-butanol and ethanol with diesel or biodiesel fuels in a constant-volume combustion chamber.* Energy, 2017. **118**: p. 613-621.

11. Hernández, J.P., Lapuerta, M., García-Contreras, R., Agudelo, J.R., *Modelling of evaporative losses in n-alcohol/diesel fuel blends..* Applied Thermal Engineering, 2016. **102**(5): p. 302-310.

12. Cadrazco, M., et al., *Genotoxicity of diesel particulate matter emitted by port-injection of hydrous ethanol and n-butanol.* Journal of Energy Resources Technology, 2017. **139**(4).

13. Lakkireddy, V.R., Mohammed, H., Johnson, J.H., *The effect of a diesel oxidation catalyst and a catalyzed particulate filter on particle size distribution from a heavy duty diesel engine.* SAE Technical Paper , 2006: p. 0148-7191, doi: 10.4271/2006-01-0877.

14. Chen, H., Mulla, S., Weigert, E., Camm, K., Ballinger, T., Cox, J., Blakeman, P., *Cold Start Concept (CSC™): A Novel Catalyst for Cold Start Emission Control.* SAE International Journal of Fuels and Lubricants, 2013. **6**(2): p. 372-381, doi:10.4271/2013-01-0535.

15. Rounce, P., Tsolakis, A., York, A.P.E., *Speciation of particulate matter and hydrocarbon emissions from biodiesel combustion and its reduction by aftertreatment.* Fuel, 2012. **96**: p. 90-99.

16. Herreros, J.M., Gill, S.S., Lefort, I., Tsolakis, A., Millington, P., Moss, E., *Enhancing the low temperature oxidation performance over a Pt and a Pt–Pd diesel oxidation catalyst.* Applied Catalysis B: Environmental, 2014. **147**: p. 835-841.

17. Chen, P., Ibrahim, U., Wang, J., *Experimental investigation of diesel and biodiesel post injections during active diesel particulate filter regenerations.* Fuel, 2014. **130**: p. 286-295.

18. Johnson, T., *Vehicular emissions in review.* SAE International Journal of Engines, 2012. **5**(2): p. 216-234, doi:10.4271/2012-01-0368.

19. Sperl, A., *The Influence of Post-Injection Strategies on the Emissions of Soot and Particulate Matter in Heavy Euro V Diesel Engine.* SAE Technical Paper , 2011. **36**(0350): p. 0336-0350, doi: 10.4271/2011-36-0350.

20. Jiao, P., Li, Z., Shen, B., Zhang, W., Kong, X., Jiang, R., *Research of DPF regeneration with NOx-PM coupled chemical reaction.* Applied Thermal Engineering, 2017. **110**: p. 737-745.

21.   Dou, D., *Application of Diesel Oxidation Catalyst and Diesel Particulate Filter for Diesel Engine Powered Non-Road Machines.* Platinum Metals Review, 2012. **56**(3): p. 144-154.

22.   Peterson, A., Lee, P., Lai, M., DiMaggio, C., *Impact of biodiesel emission products from a multi-cylinder direct injection diesel engine on particulate filter performance.* SAE Technical Paper , 2009: p. 01-1184, doi: 10.4271/2009-01-1184.

23.   Mallamo, F., Longhi, S., Millo, F., *Modeling of Diesel Oxidation Catalysts for Calibration and Control Purpose.* Int. J. Engine Res., 2013.

24.   Voltz, S.E., Morgan, C. R., Liederman, D.,, *Kinetic Study of Carbon Monoxide and Propylene Oxidation on Platinum Catalysts.* Product R&D, 1973. **12**(4): p. 294-301.

25.   Fayad, M.A., Herreros, J. M., Martos, F. J., Tsolakis, A., *Role of Alternative Fuels on Particulate Matter (PM) Characteristics and Influence of the Diesel Oxidation Catalyst.* Environmental Science & Techology, 2015. **49**(19): p. 11967-11973.

26.   Tornatore, C., Marchitto, L., Valentino, G., Iannuzzi, S., Merola, S., *Spectroscopic Investigation of Post-Injection Strategy Impact on Fuel Vapor within the Exhaust Line of a Light Duty Diesel Engine Supplied with Diesel/Butanol and Gasoline Blends.* SAE International Journal of Engines, 2013: p. 24-0066, doi:10.4271/2013-24-0066.

27.   Desantes, J., Bermúdez, V, Pastor, JV, Fuentes, E, *Investigation of the influence of post-injection on diesel exhaust aerosol particle size distributions.* Aerosol Science and Technology, 2006. **40**(1): p. 80-96.

28.   Yamamoto, K., Takada, K., Kusaka, J., Kanno, Y., Nagata, M. *Influence of diesel post injection timing on HC emissions and catalytic oxidation performance*. in *Powertrain and Fluid Systems Conference and Exhibition*. 2006.

29.   Lefort, I., Herreros, J. M., Tsolakis, A., *Reduction of low temperature engine pollutants by understanding the exhaust species interactions in a diesel oxidation catalyst.* Environmental Science & Technology, 2014. **48**(4): p. 2361-2367.

30.   Valentino, G., Iannuzzi, S., Corcione, F. E., *Experimental investigation on the combustion and emissions of a light duty diesel engine fuelled with butanol-diesel blend.* 2013, SAE Technical Paper. p. 01-0915, doi: 10.4271/2013-01-0915.

31.   Pico Technology, *8 Channel Thermocouple - Data Logger [Internet]. [Cited 3 November 2016], 2011.* vailable from URL: https://www.picotech.com/data-logger/tc-08/thermocouple-data-logger.

32.   Stein, H.J., *Diesel oxidation catalysts for commercial vehicle engines: strategies on their application for controlling particulate emissions.* Applied Catalysis B: Environmental, 1996. **10**: p. 69-82.

33.   Sukjit, E., Herreros, JM, Piaszyk, J, Dearn, KD, Tsolakis, A, *Finding synergies in fuels properties for the design of renewable fuels–Hydroxylated biodiesel effects on butanol-diesel blends.* Environmental Science & Technology, 2013. **47**(7): p. 3535-3542.

34.   Eastwood, P., *Particle Emissions from Vehicles.* John Wiley & Sons Ltd. UK., 2008.

35.   Fayad, M.A., Tsolakis, A., Fernández-Rodríguez, D., Herreros, J.M., Martos, F.J., Lapuerta, M., *Manipulating modern diesel engine particulate emission characteristics through butanol fuel blending and fuel injection strategies for efficient diesel oxidation catalysts.* Applied Energy, 2017. **190**: p. 490-500.

36.   Bobba, M., Musculus, M., Neel, W., *Effect of post injections on in-cylinder and exhaust soot for low-temperature combustion in a heavy-duty diesel engine.* SAE International Journal of Engines, 2010. **3**(1): p. 496-516, doi:10.4271/2010-01-0612.

37.   Ozsezen, A.N., Canakci, M., Turkcan, A., Sayin, C., *Effects of Biodiesel from used frying palm oil on the performance, injection, and combustion characteristics of an indirect injection diesel engine.* Energy Fuels, 2008. **22**: p. 1297-305.

38.   Chen, Z., Wu, Z., Liu, J., Lee, C., *Combustion and emission characteristics of high n-butanol/diesel ratio blend in a heavy duty diesel engine and EGR impact.* Energy Conversion and Management, 2014. **78**: p. 787-795.

39. Diehl, F., Barbier, J., Duprez, D., Guibard, I., Mabilon, G., *Catalytic oxidation of heavy hydrocarbons over Pt/Al2O3. Influence of the structure of the molecule on its reactivity.* Applied Catalysis B: Environmental, 2010. **95**(3): p. 217-227.

40. Murakami, N., N. Kojima, and M. Hashiguchi, *Oxidation of NO to NO2 in the Flue Gas (I) - Oxidation by Addition of CH3OH.* Nenryo Kyokaishi, 1982. **61**: p. 276-284.

41. Murakami, N., J. I zumi, and S. Shirakawa, *Oxidation of NO to NO2 in the Flue Gas (II) - Oxidation by Addition of H2, H2O2, CH2O, CH.* Nenryo Kyokaishi, 1982. **61**: p. 329-336.

42. Hjuler, K., Glarborg, Peter, Dam-Johansen, Kim, *Mutually promoted thermal oxidation of nitric oxide and organic compounds.* Industrial Engineering chemistry Research, 1995. **34**(5): p. 1882-1888.

43. Chong, J.J., Tsolakis, A., Gill, S.S., Theinnoi, K., Golunski, Stanislaw, E., *Enhancing the NO 2/NOx ratio in compression ignition engines by hydrogen and reformate combustion, for improved aftertreatment performance.* International Journal of Hydrogen Energy, 2010. **35**(16): p. 8723-8732.

44. Wang, W., Herreros, J.M., Tsolakis, A., York, A.P.E., *Increased NO2 concentration in the diesel engine exhaust for improved Ag/Al2 O3 catalyst NH 3-SCR activity.* Chemical Engineering Journal, 2015. **270**: p. 582-589.

45. Zhang, H.L., G.K., Boehman, A.L., Haworth, D.C. *Effects of Hydrogen Addition on NOx Emissions in Hydrogen-Assisted Diesel Combustion*. in *International Multidimensional Engine Modeling Users Group Meeting Detroit*. 2009.

46. Lilik, G.K., Zhang, H., Herreros, J.M., Haworth, D.C. and A.L. Boehman, *Hydrogen assisted diesel combustion.* International Journal of Hydrogen Energy, 2010. **35**(9): p. 4382-4398.

47. Sharma, H., Mhadeshwar, A., *A detailed microkinetic model for diesel engine emissions oxidation on platinum based diesel oxidation catalysts (DOC).* Applied Catalysis B: Environmental, 2012. **127**: p. 190-204.

48. Mudiyanselage, K., Yi, C., Szanyi, J., *Oxygen Coverage Dependence of NO Oxidation on Pt(111).* Journal of Physical Chemistry, 2009. **113**: p. 5766-5776.

49. Tighe, C.J., Twigg, M.V., Hayhurst, A.N., Dennis, J.S., *The kinetics of oxidation of diesel soots by NO2.* Combustion and Flame, 2012. **159**(1): p. 77-90.

50. Liu, S., Wu, X., Weng, D., Li, M., Ran, R., *Roles of acid sites on Pt/H-ZSM5 catalyst in catalytic oxidation of diesel soot.* ACS Catalysis, 2015. **5**(2): p. 909-919.

51. Thomas, J.F., Lewis, S.A., Bunting, B.G., Storey, J.M., Graves, R.L., Park, P.W., *Hydrocarbon selective catalytic reduction using a silver-alumina catalyst light alcohols and other reductants.* SAE International Journal, 2005: p. 0148-7191, doi: 10.4271/2005-01-1082.

52. Barro C., T.F., Obrecht P., Boulouchos K. *Influence of post-injection parameters on soot formation and oxidation in a common-rail-diesel engine using multi-color-pyrometry*. in *Conference: ASME 2012 internal combustion engine division fall technical conference*. 2012. doi: 10.1115/ICEF2012-92075.

53. Richard K., L., J. Cole, A.. *"A reexamination of the Rapre NOx process"* . Combustion and Flame, 1990. **82**(3-4): p. 435-443.

54. Shrivastava, M., Nguyen, A., Zheng, Z., Wu, H.W., Jung, H.S., *Kinetics of soot oxidation by NO2* Environmental Science & Technology, 2010. **44**: p. 4796-4801.